
Adaptive Methods for Transient Noise Analysis

Thorsten Sickenberger and Renate Winkler

Humboldt-Universität zu Berlin, Institut für Mathematik, 10099 Berlin
sickenberger/winkler@math.hu-berlin.de

Stochastic differential algebraic equations (SDAEs) arise as a mathematical model for electrical network equations that are influenced by additional sources of Gaussian white noise. In this paper we discuss adaptive linear multi-step methods for the numerical integration of SDAEs, in particular stochastic analogues of the trapezoidal rule and the two-step backward differentiation formula, together with a new step-size control strategy. Test results illustrate the performance of the presented methods.

1 Transient noise analysis in circuit simulation

Transient analysis is often performed without taking noise effects into account. But due to the parasitic effects, this is no longer possible. The increasing scale of integration, high clock frequencies and low supply voltages cause smaller signal-to-noise ratios. In several applications the noise influences the system behaviour in an essentially nonlinear way such that linear noise analysis is no longer satisfactory and transient noise analysis, i.e., the simulation of noisy systems in the time domain, becomes necessary (see [DeWi03, Wi04]). Here we deal with the thermal noise of resistors as well as the shot noise of semiconductors that are modelled by additional sources of additive or multiplicative Gaussian white noise currents that are shunt in parallel to the noise-free elements [DS98].

Thermal noise of resistors having a resistance R is caused by the thermal motion of electrons and is described by Nyquist's theorem. Hence, the associated current is modelled by additive noise,

$$i_{th} = \sqrt{\frac{2kT}{R}}\xi(t), \quad k = 1.3806 \times 10^{-23}, \quad (1)$$

where T is the temperature, k is Boltzmann's constant and $\xi(t)$ is a standard Gaussian white noise process. Shot noise of pn -junctions, caused by the

discrete nature of currents due to the elementary charge, is modelled by multiplicative noise. If the noise-free current through the pn -junction is described by a characteristic $i = g(u)$ in dependence on a voltage u , the associated Gaussian white noise current is modelled by

$$i_{shot} = \sqrt{q_e |g(u)|} \xi(t), \quad q_e = 1.602 \times 10^{-19}, \quad (2)$$

where $\xi(t)$ again is a standard Gaussian white noise process and q_e is the elementary charge. Combining Kirchhoff's Current law with the element characteristics and using the charge-oriented formulation yields a stochastic differential algebraic equation (SDAE) of the form (see [GF99] for the deterministic case)

$$A \frac{d}{dt} q(x(t)) + f(x(t), t) + \sum_{r=1}^m g_r(x(t), t) \xi_r(t) = 0, \quad (3)$$

where A is a constant singular incidence matrix determined by the topology of the dynamic circuit parts, the vector $q(x)$ consists of the charges and the fluxes, and x is the vector of unknowns consisting of the nodal potentials and the branch currents through voltage-defining elements. The term $f(x, t)$ describes the impact of the static elements, $g_r(x, t)$ denotes the vector of noise intensities for the r -th noise source, and ξ is an m -dimensional vector of independent Gaussian white noise sources (see e.g. [DeWi03, Wi04]). Hence, one has to deal with a large number of equations as well as of noise sources. Compared to the other quantities the noise intensities $g_r(x, t)$ are small.

We understand (1) as a stochastic integral equation

$$Aq(X(s)) \Big|_{t_0}^t + \int_{t_0}^t f(X(s), s) ds + \sum_{r=1}^m \int_{t_0}^t g_r(X(s), s) dW_r(s) = 0, \quad t \in [t_0, T], \quad (4)$$

where the second integral is an Itô-integral, and W denotes an m -dimensional Wiener process (or Brownian motion) given on the probability space (Ω, \mathcal{F}, P) with a filtration $(\mathcal{F}_t)_{t \geq t_0}$. The solution is a stochastic process depending on the time t and on the random sample ω . For a fixed sample ω representing a fixed realization of the driving Wiener noise, the function $X(\cdot, \omega)$ is called a realization or a path of the solution. Due to the influence of the Gaussian white noise, typical paths are nowhere differentiable.

Especially for oscillating solutions in circuit simulation one is interested in the phase noise. We aim at the simulation of solution paths that reveal the phase noise. From the solution paths statistical data of the phase as well as of moments of the solution can be computed in a post-processing step. We therefore use the concept of strong solutions and strong (mean-square) convergence of approximations.

Using techniques from the theory of DAEs as well as of the theory of stochastic differential equations (SDEs) one derives existence and uniqueness for the solutions as well as convergence results for certain drift-implicit methods for systems with index 1 DAE [Wi03].

2 Adaptive numerical methods

An efficient integrator must be able to change the step-size. We present adaptations of known schemes for SDEs that are implicit in the deterministic part (drift) and explicit in the stochastic part (diffusion) of the SDAE. Designing the methods such that the iterates have to fulfill the constraints of the SDAE at the current time-point is the key idea to adapt known methods for the SDEs to (4).

We consider stochastic analogues of the two-step backward differentiation formula (BDF₂) and the trapezoidal rule, where only the increments of the driving Wiener process are used to discretize the diffusion part. Analogously to the Euler-Maruyama scheme we call such methods multi-step Maruyama methods. The variable step-size BDF₂ Maruyama method for the SDAE (4) has the form (see [Si05] and e.g. [BuWi05] in the case of constant step-sizes)

$$A \frac{q(X_\ell) - \frac{(\kappa_\ell+1)^2}{2\kappa_\ell+1}q(X_{\ell-1}) + \frac{\kappa_\ell^2}{2\kappa_\ell+1}q(X_{\ell-2})}{h_\ell} + \frac{\kappa_\ell+1}{2\kappa_\ell+1}f(X_\ell, t_\ell) + \sum_{r=1}^m g_r(X_{\ell-1}, t_{\ell-1}) \frac{\Delta W_r^\ell}{h_\ell} - \frac{\kappa_\ell^2}{2\kappa_\ell+1} \sum_{r=1}^m g_r(X_{\ell-2}, t_{\ell-2}) \frac{\Delta W_r^{\ell-1}}{h_\ell} = 0, \quad (5)$$

$\ell = 2, \dots, N$. Here, X_ℓ denotes the approximation to $X(t_\ell)$, $h_\ell = t_\ell - t_{\ell-1}$, and $\Delta W_r^\ell = W_r(t_\ell) - W_r(t_{\ell-1}) \sim N(0, h_\ell)$ on the grid $0 = t_0 < t_1 < \dots < t_N = T$. The coefficients of the two-step scheme (5) depend on the step-size ratio $\kappa_\ell = h_\ell/h_{\ell-1}$ and satisfy the conditions for consistency of order one and two in the deterministic case and of order 1/2 in the stochastic case (see [Si05]).

A correct formulation of the stochastic trapezoidal rule for SDAEs requires more structural information (see [SiWi06]). It should implicitly realize the stochastic trapezoidal rule for the so called inherent regular SDE of (4) that governs the dynamical components. One possibility is to discretize the constraints differently, which requires the explicit knowledge of the constraints or, equivalently, a projector R along $\text{im}A$. The discrete equations

$$A \frac{q(X_\ell) - q(X_{\ell-1})}{h_\ell} + \frac{1}{2}(I - R)(f(X_\ell, t_\ell) + f(X_{\ell-1}, t_{\ell-1})) + Rf(X_\ell, t_\ell) + \sum_{r=1}^m g_r(X_{\ell-1}, t_{\ell-1}) \frac{\Delta W_r^\ell}{h_\ell} = 0, \quad (6)$$

$\ell = 1, \dots, N$, imply the correct constraints and realize the trapezoidal rule for the inherent regular SDE.

Both the BDF₂ (5) and the trapezoidal rule (6) have only an asymptotic order of strong convergence of 1/2, i.e.,

$$\|X(t_\ell) - X_\ell\|_{L_2(\Omega)} := \max_{\ell=1, \dots, N} (E|X(t_\ell) - X_\ell|^2)^{1/2} \leq c \cdot h^{1/2}, \quad (7)$$

where $h := \max_{\ell=1,\dots,N} h_\ell$ is the maximal step-size of the grid. (For additive noise the order may be 1.) This holds true for all numerical schemes that include only information on the increments of the Wiener process.

However, the noise densities given in Sec. 1 contain small parameters and the error behaviour is much better. In fact, the errors are dominated by the deterministic terms as long as the step-size is large enough [BuWi05]. In more detail, the error of the given methods behaves like $\mathcal{O}(h^2 + \varepsilon h + \varepsilon^2 h^{1/2})$, when ε is used to measure the smallness of the noise ($g_r(x, t) = \varepsilon \hat{g}_r(x, t)$, $r = 1, \dots, m$, $\varepsilon \ll 1$). Thus we can expect order 2 behaviour if $h \gg \varepsilon$.

The smallness of the noise also allows special estimates of the local error terms, which can be used to control the step-size. In [RoWi05] the authors presented a step-size control for the drift-implicit Euler scheme in the case of small noise that leads to adaptive step-size sequences that are uniform for all paths, see also [DeWi03, Wi04]. The estimates of the dominating local error term are based on values of the drift term and do not cost additional evaluations of the coefficients of the SDE or their derivatives. In [SWW06, SWW07] we extend this strategy to stochastic linear multi-step methods with deterministic order 2 and present an estimate of the mean-square local errors. Again it is based on divided differences of values of the drift term and leads to step-size sequences that are identical for all computed paths.

3 Numerical results

Here, we illustrate the potential of the step-size control strategy by simulation results for the stochastic BDF₂ applied to three test problems. For the first and the second example we use an implementation of the adaptive methods discussed in the previous section in fortran code. To be able to handle real-life problems, a slightly modified version of the schemes for MNA together with the new step-size control has been implemented in Qimonda's in-house simulator TITAN. The third example shows the performance of this industrial implementation.

A nonlinear test-SDE

First, we consider a nonlinear scalar SDE with known explicit solution. The drift and diffusion coefficients are tunable by real parameters α and β , which we have chosen as $\alpha = -10$ and $\beta = 0.01$:

$$X(t) = \int_0^t -(\alpha + \beta^2 X(s))(1 - X(s)^2) ds + \int_0^t \beta(1 - X(s)^2) dW(s), \quad t \in [0, T]. \quad (8)$$

The solution is given by

$$X(t) = \frac{\exp(-2\alpha t + 2\beta W(t)) - 1}{\exp(-2\alpha t + 2\beta W(t)) + 1}. \quad (9)$$

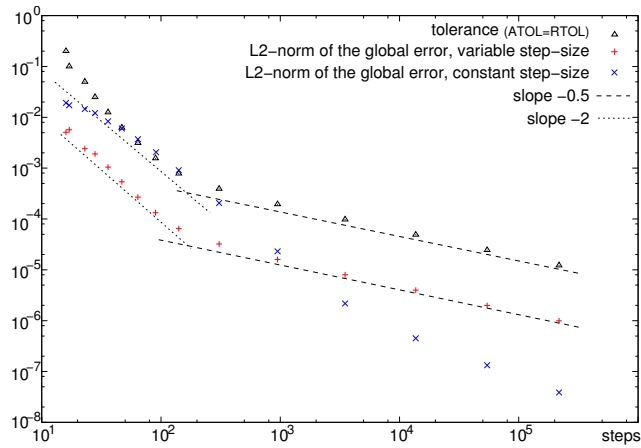


Fig. 1. Tolerance and accuracy versus steps for a test-SDE.

In Figure 1 we present a work-precision diagram. We plotted the tolerance (Δ) and the mean-square norm of the errors for adaptively chosen (+) and constant (\times) step-sizes for 100 computed paths vs. the number of steps in logarithmic scale. Lines with slopes -2 and -0.5 are provided to enable comparisons with convergence of order 2 or $1/2$. We observe order 2 behaviour up to accuracies of 10^{-4} . The results show that the proposed step-size control works very well for step-sizes above this threshold and provides considerably more accurate results than the computation with the same number of constant steps.

A MOSFET inverter circuit

Secondly, we consider a model of an inverter circuit with a MOSFET-transistor under the influence of thermal noise. The equivalent circuit diagram is given in Figure 2. The MOSFET is modelled as a current source from source to drain that is controlled by the nodal potentials at gate, source and drain.

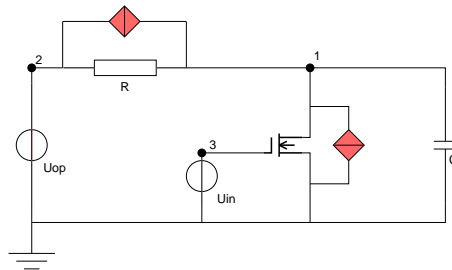


Fig. 2. Thermal noise sources in a MOSFET inverter circuit

The thermal noise of the resistor and of the MOSFET is modelled by additional white noise current sources that are shunt in parallel to the original,

noise-free elements. To make the effect of the noise more visible we scaled the noise intensities by a factor of 1000. For the simulation we used the BDF_2 with adaptively chosen step-sizes. In Figure 3 we present simulation results,

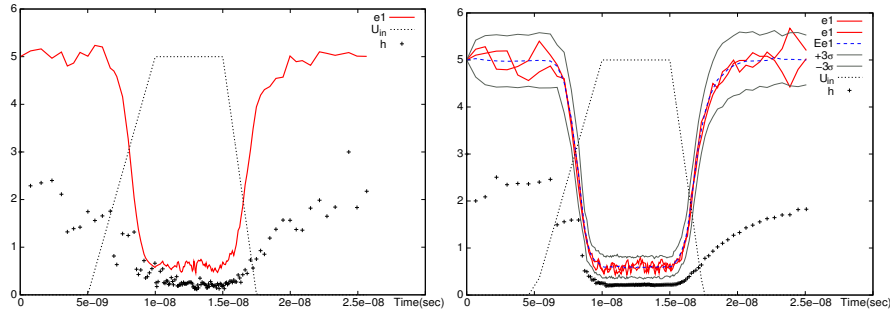


Fig. 3. Simulation results for the noisy inverter circuit:

1 path 127(+29 rejected) steps; 100 paths 134(+11 rejected) steps

where we plotted the input voltage U_{in} and values of the output voltage e_1 versus time. We compare the results for the computation of a single path (left picture) with those for the computation of 100 simultaneously computed solution paths (right picture), where the dark lines additionally show the values of two different solution paths, the dotted line gives the mean of 100 paths and the gray lines the 3σ -confidence interval for the output voltage e_1 . Moreover, the applied step-sizes, suitably scaled, are shown by means of single crosses. Using the information of an ensemble of simultaneously computed solution paths smooths the step-size sequence and reduces the number of rejected steps considerably, compared to the simulation of a single path. Also the computational cost mainly determined by the number of integration steps is reduced.

A voltage controlled oscillator

Finally, we present simulation results for a voltage controlled oscillator that has been used as a test application. It is a simplified version of a fully integrated 1.3 GHz VCO for GSM in $0.25 \mu\text{m}$ standard CMOS (see [Ti00]). For simulation, the oscillator is embedded in a test environment, using a virtual output buffer load and tuning voltage as well as core current modelled as independent DC sources. The VCO is tunable from about 1.2 GHz up to 1.4 GHz. The unknowns of the VCO in the MNA system are the charges of the six capacities, the fluxes of the four inductors, the 15 nodal potentials and the currents through the voltage sources. This circuit contains 5 resistors and 6 MOSFETs, which induce 53 sources of thermal or shot noise. To make the differences between the solutions of the noisy and the noise-free model more visible, the noise intensities had been scaled by a factor of 500.

Numerical results obtained with a combination of the BDF_2 and the trapezoidal rule are shown in Fig. 4, where we plotted the difference of the nodal

potential $V(7) - V(8)$ of node 7 and 8 versus time. The solution of the noise-free system is given by a dashed line. Four sample paths (dark solid lines) are shown. They cannot be considered as small perturbations of the deterministic solution, phase noise is highly visible. To analyze the phase noise we

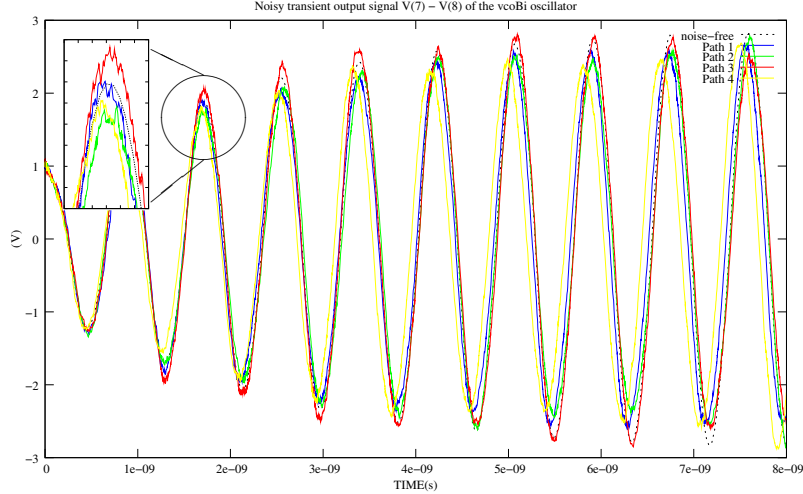


Fig. 4. Noisy transient output signal of a VCO.

repeated the simulation ten times with different initialization of the pseudo-random numbers. Then we computed the length of the first 50 periods for each solution path. On Fig. 5 the mean μ of the frequencies (horizontal lines), the smallest and the largest frequencies (boundaries of the vertical thin lines) and the boundaries of the confidence interval $\mu \pm \sigma$ (the plump lines) are presented, where σ was computed as the empirical estimate of the standard deviation. The mean appears increased and differs by about $+0.25\%$ from the noiseless, deterministic solution. Further on, the frequencies vacillate from 1.18 GHz (-0.95%) up to 1.21 GHz ($+1.55\%$). So the transient noise analysis shows that the voltage controlled oscillator runs in a noisy environment with increased frequencies and smaller phases, respectively.

References

- [BuWi05] Buckwar, E., Winkler, R.: Multi-step methods for SDEs and their application to problems with small noise. *SIAM J. Num. Anal.*, **44**(2), 779–803 (2006)
- [DS98] Demir, A., Sangiovanni-Vincentelli, A.: Analysis and simulation of noise in nonlinear electronic circuits and systems. Kluwer Academic Publishers (1998)
- [DeWi03] Denk, G., Winkler, R.: Modeling and simulation of transient noise in circuit simulation. *Mathematical and Computer Modelling of Dynamical Systems*, to appear

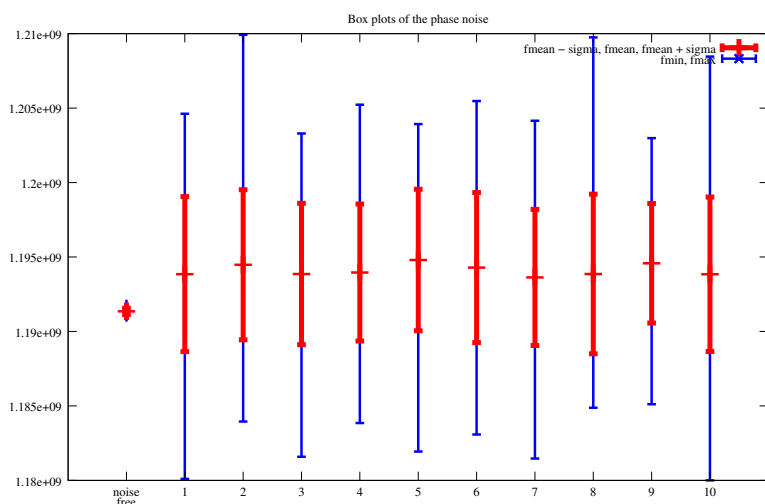


Fig. 5. Boxplots of the phase noise, scaled by a factor of 500

- [GF99] Günther, F., Feldmann, U.: CAD-based electric-circuit modeling in industry I. mathematical structure and index of network equations. *Surv. Math. Ind.*, **8**, 97–129 (1999)
- [Hi01] Higham, D.J.: An algorithmic introduction to numerical simulation of stochastic differential equations. *SIAM Review*, **43**, 525–546 (2001)
- [Ti00] Tiebout, M.: A fully integrated 1.3 GHz VCO for GSM in 0.25 μm standard CMOS with a phasenoise of -142 dBc/Hz at 3MHz offset. In: *Proceedings 30th European Microwave Conference, Paris* (2000)
- [RoWi05] Römisch, W., Winkler, R.: Stepsize control for mean-square numerical methods for stochastic differential equations with small noise. *SIAM J. Sci. Comp.*, **28**(2), 604–625 (2006)
- [Si05] Sickenberger, T.: Mean-square convergence of stochastic multi-step methods with variable step-size. *J. Comput. Appl. Math.*, to appear
- [SiWi06] Sickenberger, T., Winkler, R.: Efficient transient noise analysis in circuit simulation. In: *Proceedings of the GAMM Annual Meeting 2006, Berlin, Proc. Appl. Math. Mech.* **6**(1), 55–58 (2006)
- [SWW06] Sickenberger, T., Weinmüller, E., Winkler, R.: Local error estimates for moderately smooth problems: Part I - ODEs and DAEs. *BIT Numerical Mathematics*, to appear
- [SWW07] Sickenberger, T., Weinmüller, E., Winkler, R.: Local error estimates for moderately smooth problems: Part II - SDEs and SDAEs. In preparation
- [Wi03] Winkler, R.: Stochastic differential algebraic equations of index 1 and applications in circuit simulation. *J. Comput. Appl. Math.*, **157**(2), 477–505 (2003)
- [Wi04] Winkler, R.: Stochastic differential algebraic equations in transient noise analysis. In: *Proceedings of Scientific Computing in Electrical Engineering, September, 5th - 9th, 2004, Capo D'Orlando, Springer Series Mathematics in Industry*, 151–158 (2006)